LBL-20631 c.2

Lawrence Berkeley Laboratory

UNIVERSITY OF CALIFORNIA

RECEIVED
LAWRENCE
BERKELEY LABORATORY

MAR 6 1986

LIBRARY AND
DOCUMENTS SECTION

Materials & Molecular Research Division

Presented at the Materials Research Society
Fall Meeting, Boston, MA, December 2-7, 1985

THE STRUCTURE OF OXYGEN-IMPLANTED (111) SILICON BEFORE AND AFTER HEAT-PULSE ANNEALING

Z. Liliental-Weber, R.W. Carpenter, J.C. Kelly

October 1985

TWO-WEEK LOAN COPY

This is a Library Circulating Copy which may be borrowed for two weeks.

LBL-20631 c.2

Prepared for the U.S. Department of Energy under Contract DE-AC03-76SF00098

DISCLAIMER

This document was prepared as an account of work sponsored by the United States Government. While this document is believed to contain correct information, neither the United States Government nor any agency thereof, nor the Regents of the University of California, nor any of their employees, makes any warranty, express or implied, or assumes any legal responsibility for the accuracy, completeness, or usefulness of any information, apparatus, product, or process disclosed, or represents that its use would not infringe privately owned rights. Reference herein to any specific commercial product, process, or service by its trade name, trademark, manufacturer, or otherwise, does not necessarily constitute or imply its endorsement, recommendation, or favoring by the United States Government or any agency thereof, or the Regents of the University of California. The views and opinions of authors expressed herein do not necessarily state or reflect those of the United States Government or any agency thereof or the Regents of the University of California.

THE STRUCTURE OF OXYGEN-IMPLANTED (111) SILICON BEFORE AND AFTER HEAT-PULSE ANNEALING

Z. LILIENTAL-WEBER, and R.W. CARPENTER

Materials and Molecular Research Division, Lawrence Berkeley Laboratory, University of California, Berkeley, CA

and

J.C. Kelly

School of Physics, University of New South Wales, Australia

This work was supported by the U. S. Department of Energy under Contract No. DE-AC03-76SF00098.

THE STRUCTURE OF OXYGEN-IMPLANTED SILICON BEFORE AND AFTER HEAT-PULSE ANNEALING

Z. LILIENTAL-WEBER*, R.W. CARPENTER, and J.C. Kelly**, Center for Solid State Science and School of Engineering and Applied Science, Arizona State University, Tempe, AZ 95287
* Now at: Materials and Molecular Research Division, Lawrence Berkeley Laboratory, 62-203, University of California, Berkeley, CA 94720, under Contract No. DE-AC03-76SF00098.
** Now at: School of Physics, University of New South Wales, Australia

ABSTRACT

The structure of oxygen-implanted silicon (dose -$7.3 \times 10^{16} cm^{-2}$) has been studied by transmission electron microscopy (TEM). The as-implanted material exhibited four structurally different layers: defect-free monocrystalline silicon, amorphous silicon, monocrystalline silicon with a high defect density, and the perfect crystalline substrate. After heat-pulse annealing for 20s at 800°C, 900°C, or 1000°C, the amorphous layer recrystallized resulting in polycrystalline silicon rich in oxygen. The uniform insulator buried layer was not formed under these specific implantation and annealing conditions.

INTRODUCTION

Decreasing the device geometries in very large-scale integration (VLSI) and ultralarge-scale integration (ULSI) devices presents many challenges for the silicon technologist. Semiconductor-on-insulator (SOI) structures offer a number of advantages over standard processing in bulk silicon, thus making them one of the best prospective candidates for VLSI and ULSI devices. SOI structures formed by high-energy implantation of large doses of oxygen have attracted attention recently [1-3]. These structures consist of a nearly damage-free Si surface layer, which can be used as a substrate for epitaxial growth of Si on the top of a buried silicon oxide layer. The possibility of designing structures with different properties by changing the implantation energy, direction, dose, and dose rate makes this technique attractive. For this study we concentrated on the structure of oxygen-implanted silicon before and after annealing, and we compared these results with our recent data from nitrogen implantation performed with similar implantation conditions [4,5].

Experimental Conditions

The oxygen implantation was done at 120 keV with a dose rate of $0.6 A/cm^2$ for a total dose of $7.3 \times 10^{16} cm^{-2}$. The implantation direction was 7° from the <111> wafer normal to minimize channeling. No target heating, other than incident-beam heating was used in the experiment. We estimate that the target temperature was less than 300°C. This implantation resulted in a calculated maximum oxygen concentration of $3.5 \times 10^{21} cm^{-3}$ at a depth of 290 nm, the projected range, according to LSS theory [6].

High-resolution electron microscopy (HREM) and microanalysis were performed using a JEOL 200CX and Philips 400 ST (FEG) electron microscope fitted with a field-emission gun and Gatan electron-energy-loss spectrometer, respectively. Cross-section specimens were prepared for electron microscopy with the beam direction along <110>, <100> and <112>. The structure of the interface was investigated by the lattice imaging of (111), (200), and (220) planes of 0.31 nm, 0.27 nm, and 0.2 nm spacing, respectively.

Annealing treatment was carried out in Ar ambient in a Heat-pulse apparatus consisting of a water-cooled reflective chamber containing upper and lower banks of tungsten halogen lamps. The stationary Si wafer, positioned equidistant between the lamp arrays was heated rapidly at 100°C/sec with up to 20kW of radiant energy trapped between the reflectors. The temperature was measured by a thermocouple attached to the Si wafer on which the samples were placed.

Results

1. Structure of as-implanted wafers

The as-implanted material exhibited four structurally different layers (Fig. 1a). Going inward from the ion-incident surface, the first layer (I) was defect-free monocrystalline silicon 15 nm thick (Fig. 1b). The second layer (II) was amorphous silicon 190 nm thick. The third layer (III) was crystalline Si 100 nm thick, containing many lattice defects (Fig. 1c). The fourth layer (IV) was the perfect crystal substrate.

The interface between the amorphous layer and the crystalline Si layer with defects was quite undulated with a wave amplitude ~5 nm. Microdiffraction and microelectron-energy-loss spectroscopy (10 nm incident probe size) showed an oxygen gradient and a difference in short-range order across the amorphous layer (II), with the highest oxygen content near the interface with the silicon crystalline layer (III).

An example of the crystalline-defect layer is shown in Fig. 1c. Two types of defects were observed: faulted loops with diameter 15-20 nm on {111} planes mainly 200-300 nm for the incident surface, and extended defects on {113} planes along <110> direction 300-350 nm from the incident surface. These last defects appear to be at most 1 nm thick, and their density is very low compared with the same kind of defects observed in nitrogen-implanted samples (Fig. 2).

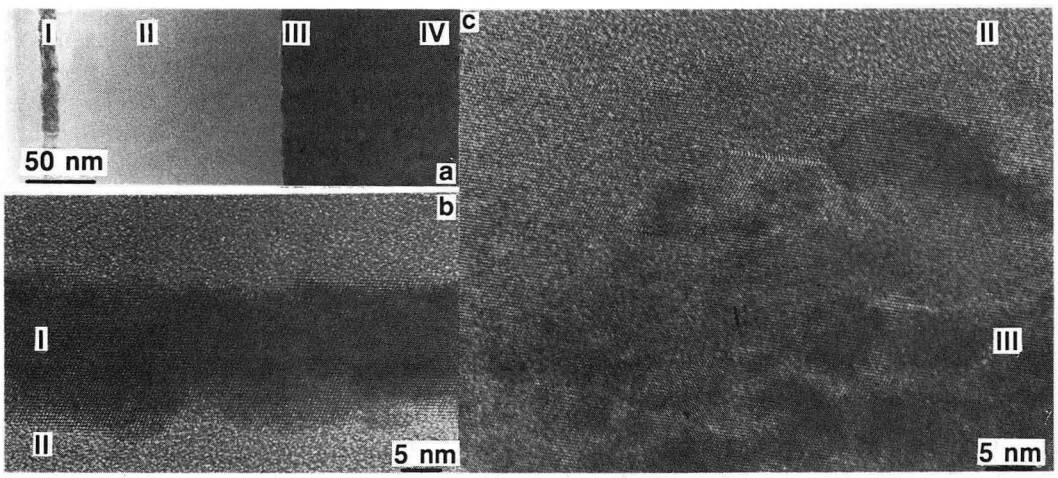

(a-XBB 8511-9667; b-XBB 8511-9668; and, c-XBB 8511-9669)

Fig. 1. The structure of an as-implanted sample:
a) cross-section sample; four different layers are present,
b) monocrystalline Si surface (I),
c) interface between the amorphous layer (II) and the crystalline layer (III); loops on {111} planes are visible in the defected layer (III).

2. Structure of heat-pulse annealed samples (1000°C for 20s)

It can be easily observed from convergent beam electron diffraction (CBED) patterns that recrystallization started from both crystalline surfaces and followed the orientation of the bounding substrate, but the recrystallization was not uniform. Other grains with random orientations were observed. The sizes of these grains diminished toward the middle of the formerly amorphous layer. The quality of regrowth can be observed easily from the sharpness of the first-order Laue zone (folz) on the CBED pattern. Such patterns, taken near the former interfaces of both the surface monocrystalline layer (I) and the crystalline defect layer (III), show a "folz" line blurred only slightly (Fig. 3b) compared to the "folz" line from a perfect substrate (IV). The "folz" line is completely blurred when the CBED patterns were taken from the middle of the formerly amorphous layer (II) (Figs. 3c and 3d). This blurred "folz" line suggests the existence of randomly oriented small grains and presence of high defect density. Indeed HREM images from different areas of the re grown amorphous layer confirm this observation. The regrown Si with the substrate orientation is followed by the imbedded grains of random orientation.

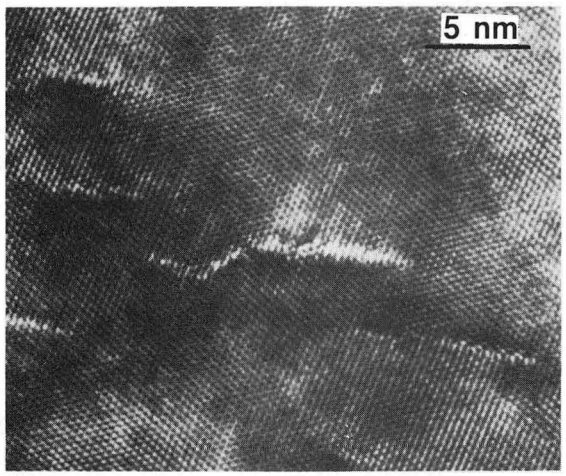

Fig. 2. {113} defects in a nitrogen-implanted sample. XBB 8511-9666

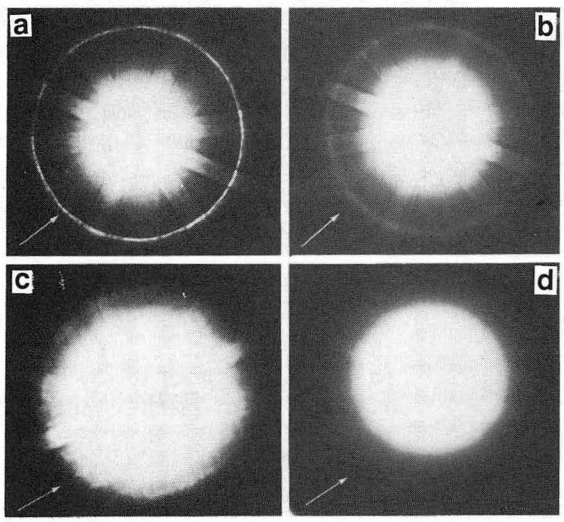

Fig. 3. CBED pattern from the recrystallized amorphous layer (annealing for 20s at 1000°C): a) sharp "folz" line from the perfect crystalline layer, b) slightly diffused "folz" line from the regrown area close to the interface with the crystalline layer, c) and d) middle of the formerly amorphous layer - "folz" line hardly visible. XBB 8511-9665

The size of these grains is larger near both crystalline interfaces Fig. 4 (a) and smaller in the middle of the formerly amorphous layer Fig. 4 (b). From the spacing characteristic for (111) Si, one can conclude that polycrystalline silicon is formed. In the middle of the amorphous layer (~120 nm from the incident surface), small silicon grains (2-5 nm diameter) are imbedded in the amorphous material. Energy-loss spectra taken from the different areas of the sample show the presence of oxygen in the former amorphous layer (II), with a slight shift of oxygen maximum concentration toward the middle of the layer. The silicon L-edge and the oxygen K-edge after standard-power low-background stripping are shown in Fig. 5a and 5b. In the crystalline defective layer, the number of faulted

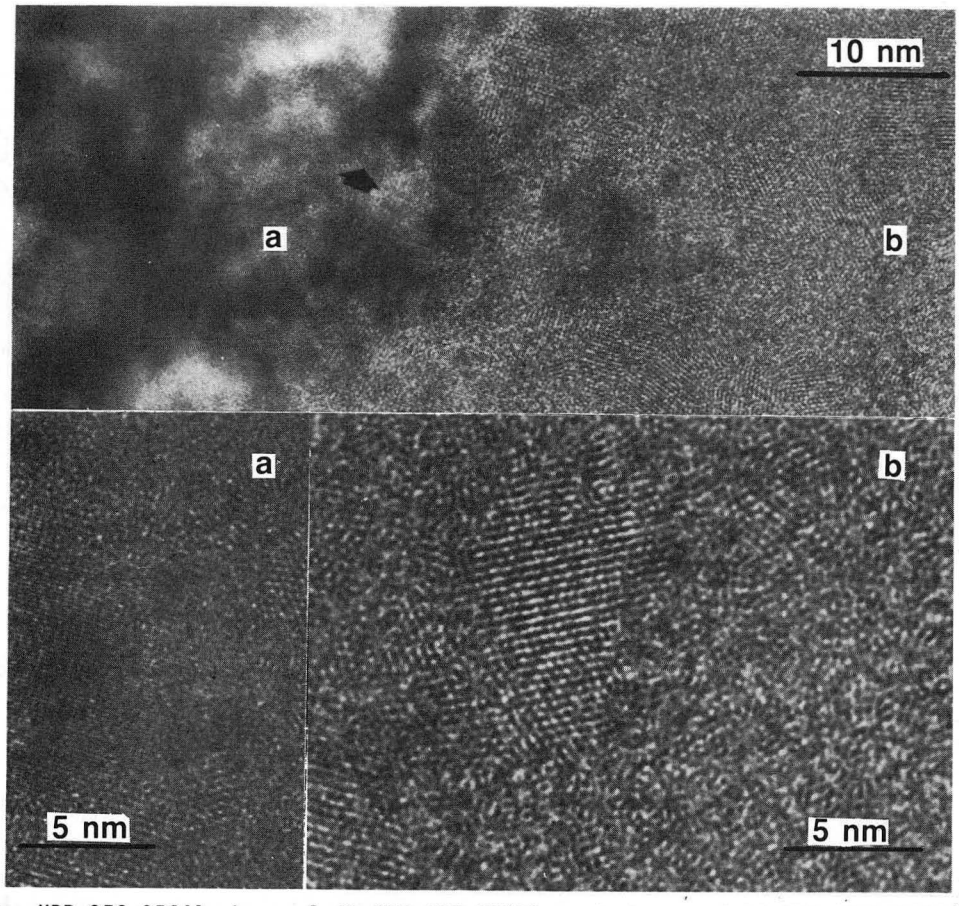

(Top-XBB 850-9564A; Lower left-XBB 850-9563A; and, Lower right-XBB 850-9565A)

Fig. 4. Structure of the regrown amorphous layer; marked areas mean:
(a) close to the interface with the crystalline layer,
(b) in the middle of the formerly amorphous layer. Higher magnification of marked areas are shown, respectively.

loops on the {111} planes is slightly increased upon annealing, and the {113} defects were no longer observed.

The sample structure after heat-pulse annealing for 20 sec at 800°C is similar to the structure described above. The recrystallized Si grains are slightly smaller on the both interfaces with crystalline Si. The middle part of formerly amorphous layer remains amorphous after annealing, at 800°C.

Discussion

Pulse annealing, commonly used to produce solid-phase regrowth of amorphized layers in implanted Si, resulted in the present case in regrowth of polysilicon rich in oxygen. Figures 3 and 4 show, that, with the present implantation condition and annealing treatment, no continuous insulating SiO_2 film was formed, as required for SOI technology. However, the monocrystalline Si surface layer allows the Si layer needed for the SOI process to regrow. A few {113} defects observed in the as-implanted sample were not found after the annealing due either to their disappearance or to their low density.

The disappearance of the {113} defects was definitely observed in nitrogen-implanted samples after heat-pulse annealing. They were unstable under annealing at 900°C or more. These defects have been studied intensely [7-10] and their interpretation vary widely. They have been attributed to transition metals, or to carbon, or oxygen decoration of {113} faults, and they have also been interpreted as rod-shaped impurity precipitates. Their high density after nitrogen implantation makes it reasonable to suppose that they may contain nitrogen as well as silicon. The low density of {113} defects observed in this study and by others may suggest that some nitrogen impurities are often present either in an ion implantation beam or in the Si target. After high dose bombardment the metastable {113} defects can be formed. Further study is necessary to understand the details of those defects as well to define the proper implantation and annealing condition for SOI devices.

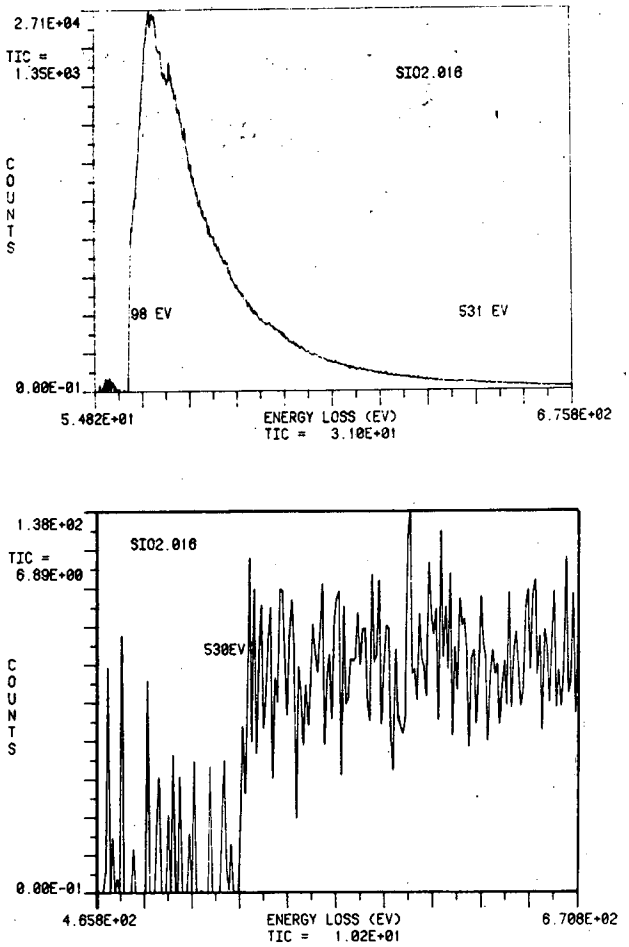

Fig. 5. Electron energy-loss spectra taken from the middle of the formerly amorphous layer ~120 nm from the intrance surface: a) Si L-edge b) oxygen K-edge.

Acknowledgment

This work was supported by NSF-DMR-831049 and was done at the High Resolution Electron Microscopy Facility in the Center for Solid State Science at Arizona State University.

References

1. R.A. Moline and A.G. Cullis, Appl. Phys. Lett. 26, 551 (1975)
2. R. W. Carpenter, Ultramicroscopy 8, 79 (1982).
3. D. Fathy, O.L. Krivanek, R.W. Carpenter and S.R. Wilson, Inst. Phys. Conf. Ser. No. 67, 479 (1983).
4. Z. Liliental, R.W. Carpenter, D. Fathy and J.C. Kelly, Mat. Res. Symp. Proc. Vol. 25, 525 (1984).
5. Z. Liliental, R.W. Carpenter and J.C. Kelly, Thin Solid Film in press.
6. J.F. Gibbons, W.S. Johnson and S.W. Mylroie, "Projected Range Statistics for Semiconductor and Related Materials", published by Dowdon Hutchinson and Ross Inc. Stroudsburg, PA (1975) distributed by Academia Press.
7. L.G. Sallisbury and M.H. Loretto, Phil. Mag. A 39, 317 (1979).

8. T.Y. Tan, H. Foell, S. Mader and W. Krakow, Mat. Res. Symp. Proc. Vol. 2, 179 (1981).
9. M. Pasemann, D. Hoehl, A.L. Aseev and P. Pchelyokow, Phys. Stat. Sol. (a) 80, 135 (1983).
10. H. Bartsch, D. Hoehl and G. Kastner, Phys. Stat. Sol. (a) 83, 543 (1984).

This report was done with support from the Department of Energy. Any conclusions or opinions expressed in this report represent solely those of the author(s) and not necessarily those of The Regents of the University of California, the Lawrence Berkeley Laboratory or the Department of Energy.

Reference to a company or product name does not imply approval or recommendation of the product by the University of California or the U.S. Department of Energy to the exclusion of others that may be suitable.

LAWRENCE BERKELEY LABORATORY
TECHNICAL INFORMATION DEPARTMENT
UNIVERSITY OF CALIFORNIA
BERKELEY, CALIFORNIA 94720